ARTICLE
Journal of Cellular Biochemistry 106:1031–1040 (2009)

Journal of Cellular Biochemistry

Cholesterol-Regulated Stress Fiber Formation

Maosong Qi,[1] Yuzhen Liu,[1] Michael R. Freeman,[2,3,4] and Keith R. Solomon[1,2,5*]

[1]*Department of Orthopaedic Surgery, Harvard Medical School, 300 Longwood Avenue, Boston, Massachusetts 02115*

[2]*Department of Urology, Children's Hospital Boston, Harvard Medical School, 300 Longwood Avenue, Boston, Massachusetts 02115*

[3]*Department of Surgery, Harvard Medical School, 300 Longwood Avenue, Boston, Massachusetts 02115*

[4]*Department of Biological Chemistry and Molecular Pharmacology, Harvard Medical School, 300 Longwood Avenue, Boston, Massachusetts 02115*

[5]*Department of Orthopaedic Surgery, Harvard Medical School, 300 Longwood Avenue, Boston, Massachusetts 02115*

ABSTRACT

Dynamic interactions between cellular membranes and the cytoskeleton are known to play major roles in many cellular responses to environmental cues. External signals resulting in proliferation, differentiation, polarization, and motility must be translated from chemical signals into changes of state, often involving the cytoskeleton-dependent altering of cell shape and redistribution of molecules. Cholesterol, a critical component of eukaryotic cell membranes, performs vital roles in regulating membrane dynamics and function. Here we demonstrate, using mesenchymal and epithelial cell lines, that depletion of membrane cholesterol results in Src kinase-mediated Rho activation and caveolin phosphorylation, which together collaborate to form stress fibers. These results demonstrate that cholesterol is a critical regulator of membrane-cytoskeletal dynamics and suggest that altered cholesterol concentrations may result in dramatic changes in cellular responses mediated by the cytoskeleton. J. Cell. Biochem. 106: 1031–1040, 2009.

KEY WORDS: CHOLESTEROL; STRESS FIBER; RHO; ROCK; SRC; CAVEOLIN-1

Cholesterol is a critical component of eukaryotic cell membranes, with important effects on membrane fluidity, stiffness, molecular transport processes, and on the arrangement of membranes into various macro and microdomains, including lipid rafts [Mukherjee and Maxfield, 2004; Simons and Vaz, 2004]. All of these processes require or result in interactions between the peripheral membrane and the underlying cytoskeleton. How cholesterol contributes to the interaction between the membrane and the cytoskeleton is only now beginning to emerge. For instance, Lillemeier et al. [2006] have demonstrated that most membrane proteins are found in cholesterol-enriched regions of the membrane that require actin anchors for maintaining their proper composition and distribution [Lillemeier et al., 2006]. Sun et al. [2007] showed that adhesion energy between the membrane and cytoskeleton as measured by atomic force microscopy was directly correlated with membrane cholesterol levels. In that report, they demonstrated that increased cholesterol strengthened, while reduced cholesterol lessened the adhesion energy [Sun et al., 2007]. Others have shown that lipid rafts including caveolae, which are membrane microdomains that contain high concentrations of cholesterol and sphingolipids, have a reciprocal regulatory interaction with the cytoskeleton. In total these reports demonstrate that the actin cytoskeleton regulates the function of specialized lipid rafts [van Deurs et al., 2003], while lipid raft localized proteins regulate the cytoskeleton [Green et al., 1999; Michaely et al., 1999; Skubitz et al., 2000; Thorne et al., 2000; Hocking and Kowalski, 2002; Leitinger and Hogg, 2002; Baron et al., 2003; MacLellan et al., 2005] (reviewed in Maxfield [2002]).

These robust dynamics between the cholesterol-enriched lipid rafts and the cytoskeleton are consistent with roles demonstrated for

Abbreviations used: BSA, bovine serum albumin; CHX, cycloheximide; Erk, extracellular signal-regulated kinase; EDTA, ethylenediaminetetraacetic acid; EGTA, ethylene glycol tetraacetic acid; FA, focal adhesions; GDP, guanosine diphosphate; GTP, guanosine triphosphate; MβCD, methyl-β-cyclodextrin; MLB, Mg2+ lysis buffer; PBS, phosphate-buffered saline; PMSF, phenylmethylsulfonyl fluoride; RIPA, radioimmunoprecipitation assay; ROCK, Rho kinase; SDS–PAGE, sodium dodecyl sulfate–polyacrylamide gel electrophoresis.

Grant sponsor: National Institutes of Health grant; Grant number: CA101046.

*Correspondence to: Keith R. Solomon, PhD, Department of Orthopaedic Surgery, Children's Hospital Boston, Enders 1030, 300 Longwood Avenue, Boston, MA 02115. E-mail: keith.solomon@childrens.harvard.edu

Received 7 November 2008; Accepted 7 January 2009 • DOI 10.1002/jcb.22081 • 2009 Wiley-Liss, Inc.

Published online 19 February 2009 in Wiley InterScience (www.interscience.wiley.com).

rafts in establishing and maintaining cell polarity [Gomez-Mouton et al., 2001; Manes et al., 2001], as well as in regulating cell size and shape [Lee et al., 2002; Park et al., 2002; Woodman et al., 2002; Naal et al., 2003; del Pozo et al., 2004]. Consistent with this view, a recent report described a central, specific role for lipid rafts in cytoskeletal regulation, in which Rac1, a membrane proximal GTPase, is necessarily directed to raft membranes as part of the process by which cell extensions are formed [del Pozo et al., 2004]. Thus, through a variety of indirect mechanisms, membrane cholesterol has been recognized as exerting a regulatory function on the cytoskeleton.

The connection between the plasma membrane and the cytoskeleton is likely pivotal to understanding how cells convert information conveyed by mechanical forces into signal transduction cascades. Many cells, including osteoblasts (as used in these studies), experience mechanical forces through hydrostatic pressure and cyclic stretch [Hughes-Fulford, 2004; Scott et al., 2008]. One consequence of applying mechanical forces to cells is the formation of stress fibers, a response that is necessary to resist and reduce stress and strain [Pellegrin and Mellor, 2007]. Information flow from the peripheral membrane into cells in response to mechanical force is, at least in part regulated by membrane cholesterol [Meazzini et al., 1998; McGarry et al., 2005; Faure et al., 2008]. However, the mechanism by which cholesterol exerts its action in stress fiber formation is obscure. Prior studies have demonstrated the Rho GTPase is a major regulator of actin polymerization [Pellegrin and Mellor, 2007]. Other studies have demonstrated that Src family kinases phosphorylate caveolin (the structural protein of the caveolar type of lipid raft), which is then directed to focal adhesions [Li et al., 1996b; Volonte et al., 2001; Sanguinetti et al., 2003; Labrecque et al., 2004; Zhang et al., 2007]. In our current report we demonstrate that membrane cholesterol directly regulates actin stress fiber formation via a Rho-, Src-, and caveolin-dependent mechanism.

MATERIALS AND METHODS

MATERIALS

Methyl-β-cyclodextrin (MβCD) and water soluble cholesterol (CHL) were purchased from Sigma (St. Louis, MO). Anti-phospho-Erk, anti-Erk, and anti-phospho-Src (Tyr416, or Tyr527) monoclonal antibodies as well as MEK1/2 inhibitor U0126 were obtained from Cell Signaling Technology (Danvers, MA). Monoclonal anti-phospho-Cav1 (pY14) and polyclonal anti-Cav1 were purchased from BD Transduction Laboratories (San Jose, CA). Actin polymerization inhibitor latrunculin A (Lat A) was purchased from Molecular Probes (Invitrogen, Carlsbad, CA). Src inhibitor PP2 was obtained from Calbiochem (San Diego, CA). siRNA and scrambled RNA were purchased from Ambion (Austin, TX).

CELL CULTURE

The MC3T3-E1 mouse osteoblast cell line [Sudo et al., 1983] (referred to as MC3T3), and the PC3 human prostatic adenocarcinoma cell line were purchased from the American Type Culture Collection (ATCC; Manassas, VA). MC3T3 cells were cultured in α Minimum Essential Medium; PC3 cells were cultured with Dulbecco's Modified Eagle's Medium at 37°C in 5% CO_2. All media were supplemented with 2 mM L-glutamine, 1 mM sodium pyruvate and 10% fetal calf serum.

CHOLESTEROL DEPLETION/REPLETION

Cells grown on plastic culture dishes or on coverslips were incubated in serum-free medium (O.N. 37°C in 5% CO_2) and cholesterol was depleted by treatment with MβCD (5 mM). After incubation at 37°C for different times (see figures), cells were washed with PBS and fixed with 4% paraformaldehyde for fluorescent staining, or lysed in MLB or RIPA buffer for protein analyses. In some experiments cholesterol was repleted prior to fixation by incubating cells in water soluble cholesterol (15 μg/ml) for 90 min at 37°C in 5% CO_2.

IMMUNOFLUORESCENT AND ACTIN STAINING

Cells were seeded on coverslips in 3-cm Petri dishes, cultured (O.N. 37°C in 5% CO_2), and treated with MβCD or were mock treated. After treatment, cells were washed with PBS, and then fixed with 4% paraformaldehyde in PBS for 30 min at room temperature (RT). Cells were permeabilized with 0.1% Triton X-100/PBS for 5 min, then blocked with 2% BSA for 1 h at RT. Primary antibodies were added in PBS at 1:500 and incubated at RT for 90 min. After washing (4× with PBS), FITC-coupled reporter antibodies in PBS containing phalloidin-rhodamine were added, and the cells incubated at RT for 60 min in the dark with mild shaking. After washing (4× with PBS), the slides were mounted with Vectashield (Vector Laboratories, Burlingtgame, CA) and processed for microscopy.

CELL LYSIS AND IMMUNOBLOTTING

MC3T3 cells were grown in 3-cm dishes. After treatments, cells were rinsed twice with ice-cold PBS then lysed with RIPA buffer (50 mM Tris, pH 7.4, 150 mM NaCl, 1% NP-40, 0.5% Sodium deoxycholate, 0.1% SDS, 5 mM EDTA, 1 mM EGTA, with 0.2 mM sodium orthovanadate, 0.2 mM PMSF and mixed protease inhibitor tablet (Roche Diagnostics, Basel, Switzerland)). Cells were scraped, transferred to 1.5 ml tubes, and passed six times through 26-gauge needle. Lysates were cleared by centrifuge at 10,000*g*, 4°C for 15 min in a microcentrifuge.

GTPASE ASSAY

Rho-GTP activity was assayed by using EZ-Detect™ Rho activation kit (Pierce, Rockford, IL). MC3T3 cells grown in 10-cm dishes were serum starved (O.N. 37°C in 5% CO_2) and treated with 5 mM MβCD for 0, 30, and 60 min. Cells were washed (2× ice-cold PBS) then lysed in MLB buffer (25 mM Hepes, pH 7.5, 150 mM NaCl, 1% Igepal CA-630, 10% glycerol, 25 mM NaF, 10 mM $MgCl_2$, 1 mM EDTA, 1 mM sodium orthovanadate and protease inhibitor cocktail). GTPase activation was assayed following the manufacture's instructions. Briefly, 10 μg of RhoA assay reagent was added to 1 ml (800 μg) of lysate and rotated at 4°C for 60 min. Two assay controls containing either GDP (negative control) or GTPγS (positive control) were performed in parallel. After incubation, assay beads were washed (3× with MLB) and boiled with in SDS containing sample buffer for 5 min. Samples were resolved by SDS–PAGE using a 12% polyacrylamide gel, electrotransferred to nitrocellulose and immunoblotted with an anti-RhoA antibody.

RESULTS

In order to begin to understand how membrane cholesterol affects the actin cytoskeletal dynamics two different cell lines, MC3T3 murine osteoblasts and PC3 human prostatic adenocarcinoma cells, were treated with methyl-β-cyclodextrin (MβCD) for 30 or 90 min to deplete membrane cholesterol. Staining of MC3T3 cells with rhodamine-phalloidin indicated that cholesterol depletion progressively increased the apparent length and thickness of stress fibers (Fig. 1A), in a process that required no new protein synthesis as judged by the failure of cycloheximide (CHX) treatment to inhibit stress fiber formation (Fig. 1B). PC3 cells demonstrated a ''rounding'' phenomenon after MβCD treatment, but here too rhodamine-phalloidin staining revealed that this treatment also increased the length and thickness of apparent stress fibers (Fig. 1C).

Since caveolin-1 (Cav1) is an abundant cholesterol binding/transport protein [Murata et al., 1995; Uittenbogaard and Smart, 2000; Sleer et al., 2001; Frank et al., 2006] that is known to interact with actin, we next assessed the effect of acute cholesterol depletion on Cav1. Given that PC3 and MC3T3 cells were similarly affected by MβCD treatment, but MC3T3 cells remained well attached to culture flasks/dishes/coverslips, we further examined the mechanism of stress fiber formation using MC3T3 cells. The cellular distribution of Cav1 and phosphorylated caveolin-1 (p-Cav1) were analyzed by staining MC3T3 cells with anti-caveolin and anti-phospho-caveolin-1 antibodies, respectively. These immunofluorescent imaging studies indicated that the majority of Cav1 in control cells was perinuclear and cytosolic, with little on the cell surface (a phenomenon already noted for cells in culture [Smart et al., 1994; Conrad et al., 1995; Thyberg et al., 1997]). However, cholesterol depletion caused a modest redistribution of Cav1 toward the plasma membrane (Fig. 2A). In contrast, p-Cav1 was found in abundance on the plasma membrane at, or near, apparent focal adhesions; treatment with MβCD further enhanced this distribution of p-Cav1, and appeared to decorate each stress fiber with p-Cav1 at the fiber ends (Fig. 2B). The appearance of p-Cav1 at the ends of the stress fibers could be caused by either a redistribution of p-Cav1 to the focal adhesions, an increase in p-Cav1 levels, or both. To assess whether there was an increase in p-Cav levels after MβCD treatment, mock and MβCD treated MC3T3 cells were analyzed by immunoblot

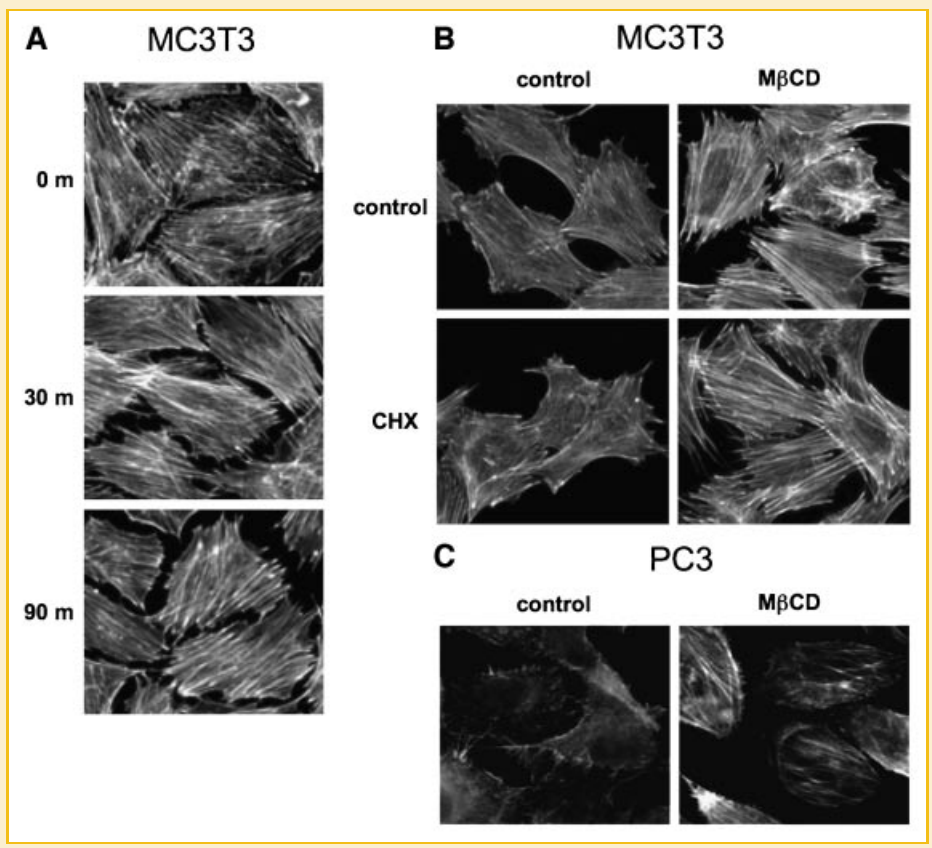

Fig. 1. Cholesterol depletion by MβCD induces stress fiber formation. A: Treatment time course. MC3T3 cell were seeded onto coverslips in 3-cm dishes and cultured 1–2 days. Cells were then serum starved overnight. MβCD was added to the medium at a final concentration of 5 mM for the indicated times. Cells were then fixed with 4% paraformaldehyde, permeablized in 0.1% Triton X-100, and stained with rhodamine-phalloidin to visualize actin. B: MβCD-induced stress fiber formation does not require de novo protein synthesis. Serum-starved MC3T3 cells were treated with 10 μg/ml cycloheximide (CHX) for 60 min, followed by treatment with 5 mM MβCD for 30 min. Stress fibers were then visualized as described in (A). C: PC3 cell were seeded onto coverslips in 3-cm dishes and cultured 1–2 days. Cells were then serum starved overnight. MβCD was added to the medium at a final concentration of 5 mM for 30 min. Stress fibers were then visualized as described in (A).

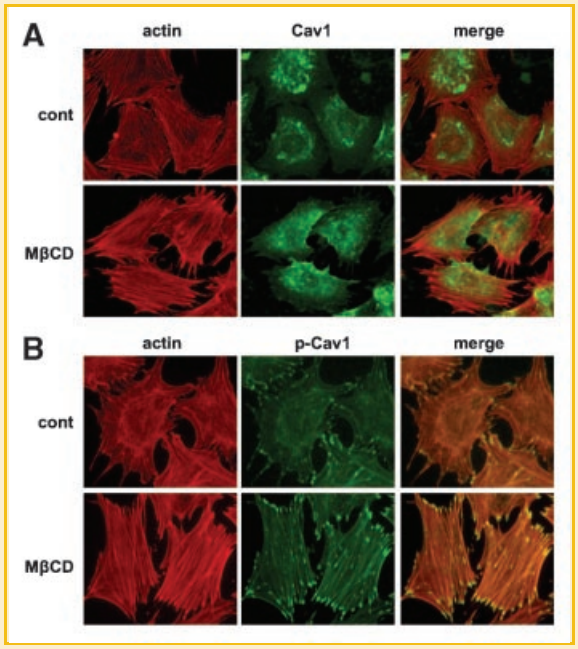

Fig. 2. MβCD treatment induces caveolin and phosphorylated-caveolin redistribution. A: Redistribution of Cav1 by MβCD. Serum-starved MC3T3 cells were treated with 5 mM MβCD for 30 min. Cells were fixed, permeablized and blocked with 2% BSA. Polyclonal anti-Cav1 antibody was added at 1:500 in PBS and incubated for 90 min at RT. After washing with PBS, FITC-coupled goat anti-rabbit antibody plus rhodamine-phalloidin were added and incubated for 60 min in the dark. B: MβCD-induced p-Cav1 distribution. MC3T3 cells were treated as in (A). After blocking with BSA, cells were stained with monoclonal anti-phospho-Cav followed by a FITC-coupled goat anti-mouse reporter antibody.

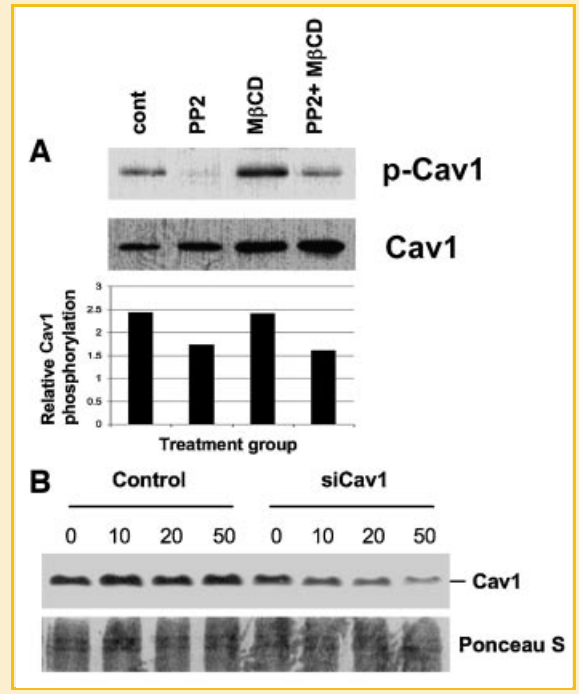

Fig. 3. Caveolin-1 and phosphorylated caveolin are required for cholesterol-depletion induced stress fiber formation. A: Cholesterol depletion does not induce Cav1 phosphorylation. MC3T3 cells were serum-starved and were mock treated (lanes 1 and 2), or were treated with 5 mM MβCD for 30 min (lanes 3 and 4). In some cases (lanes 2 and 4) cells were pre-treated with 10 μM PP2 for 30 min. After treatments cells were washed with cold PBS and lysed in RIPA buffer. Thirty micrograms of total protein from each lysate was subjected to immunoblot analysis with monoclonal anti-p-Cav1 and HRP-coupled anti-mouse reporter antibodies. To detect caveolin, the membrane was stripped, blocked again with BSA, and blotted with polyclonal anti-Cav1 antibody. The lower panel is a plot of relative caveolin-1 phosphorylation versus treatment group based on the densitometry of the phospho-caveolin and caveolin signals. B: Targeting Cav1 by siRNA greatly reduces Cav1 protein level. MC3T3 cell grown in 3-cm cell culture dishes (80% confluent) were transfected with scrambled RNA or siCav1 at 0, 10, 20, and 50 nM, using Lipofectamine 2000. Cells were cultured for 24 h and lysed in RIPA buffer. Thirty micrograms of total protein of each sample was subjected to immunoblot analysis using polyclonal anti-Cav1 and HRP-coupled anti-rabbit reporter antibody. Staining the membrane with ponceau S was used to indicate that each gel lane was equally loaded/transferred. C: Knockdown of Cav1 suppresses stress fiber formation. MC3T3 cells grown on coverslips in 3-cm cell culture dishes (50% confluent) were transfected with scrambled RNA or siCav1 at 50 nM, using Lipofectamine 2000. Cells were cultured for 24 h, starved overnight and then treated with 5 mM MβCD for 30 min. After fixation, cells were permeablized and blocked with 2% BSA. Polyclonal anti-Cav1 antibody (Top panel) or monoclonal anti-phospho-caveolin (Bottom panel) was added and incubated for 90 min at RT. After washing with PBS, FITC-coupled goat anti-rabbit reporter antibody plus rhodamine-phalloidin were added and incubated in dark for 60 min.

(Fig. 3A, lane 3). This analysis indicated that MβCD treatment did not cause an increase in the amount of p-Cav1 relative to the level of total Cav1, suggesting that the major effect of MβCD treatment, with respect to Cav1 was to redistribute the protein to the cell surface.

The role of Cav1 in stress fiber formation was further assessed through the use of Cav1 targeted siRNA oligonucleotides. Treatment with Cav1 siRNA (50 nM) resulted in a reduction in Cav1 protein >90% as determined by immunoblot analysis (Fig. 3B). Use of the Cav1 specific siRNA at this concentration prevented nearly all of the stress fiber formation induced by cholesterol depletion (Fig. 3C), suggesting that Cav1 is an obligate component of cholesterol-regulated stress fiber formation.

Stress fiber assembly is controlled by the action of Rho family GTPases, specifically RhoA [Pellegrin and Mellor, 2007]. We hypothesized that cholesterol depletion triggered RhoA GTPase activation, and tested this hypothesis by assessing the ability of MβCD treatment to activate RhoA (Fig. 4A). From the results obtained it is apparent that MβCD treatment substantially increased the level of GTP bound RhoA (activated RhoA) after 30 min, an effect that continued to increase up to 60 min of treatment. Interestingly, the level of total RhoA decreased (see lysate RhoA panel in Fig. 4A), indicating that not only is GTP-bound RhoA increased, but that its proportion to the total RhoA is further enhanced by the down regulation of total RhoA.

Downstream of RhoA is Rho-kinase (ROCK), a serine/threonine kinase which is activated by Rho binding, leading to prominent stress fiber formation [Pellegrin and Mellor, 2007]. We tested the involvement of ROCK, by using a specific ROCK inhibitor, Y27632, and examining its effect on cholesterol depletion-mediated stress fiber formation (Fig. 4B). Y27632 treatment prevented MβCD treatment-induced stress fiber formation.

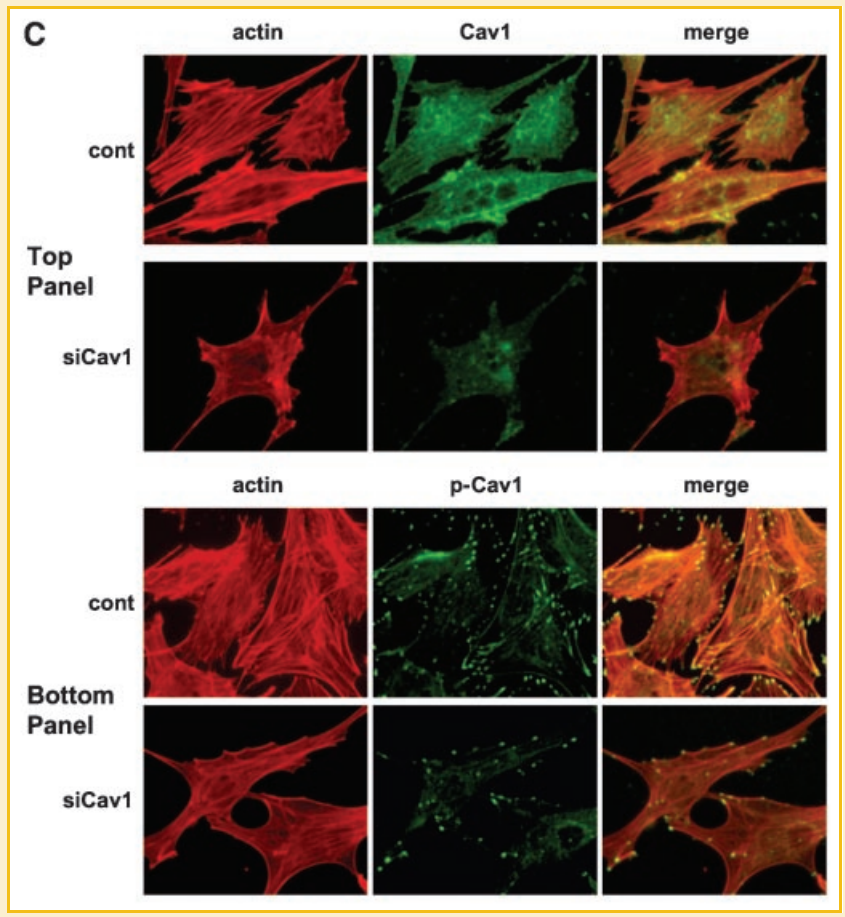

Fig. 3. (*Continued*).

Given the critical role of Cav1 in stress fiber formation, and the apparent localization of p-Cav1 to the ends of the stress fibers we sought to determine whether Cav1 phosphorylation was required for stress fiber formation. Src kinase lies upstream of Cav1 phosphorylation and is known to phosphorylate Cav1 on Tyr-14 (the site recognized by the p-Cav1 antibody used in these studies). To examine the role of Src in cholesterol-depletion induced stress fiber formation we first tested whether cholesterol depletion activated Src (Fig. 5A). Src activity is controlled by phosphorylation, including autophosphorylation at two tyrosines, Y-416 in the activation loop, and at Y-527, a Src kinase inhibition site. To examine Src activation, we subjected MβCD-treated and mock-treated cells to immunoblot analysis using antibodies recognizing either pY-416 or pY-527 (Fig. 5A). These results demonstrate that MβCD treatment increased phosphorylation at Y-416, and very modestly reduced phosphorylation at Y-527, a result consistent with Src kinase activation. Next we assessed the role of Src kinase activity in MβCD-induced stress fiber formation by testing the effect of the specific Src family kinase inhibitor, PP2, on stress fiber formation and Cav1 phosphorylation (Figs. 3A and 5B). These results indicated that inhibition of Src blocked Cav1 phosphorylation (Figs. 3A, lanes 2 and 4 and 5B) as well as stress fiber formation (Fig. 5B).

Whether activation of Src was upstream or downstream of RhoA activation was tested using PP2 (Fig. 4A, lanes 4 and 5). We observed that the inhibition of Src blocked MβCD-induced RhoA activation, strongly suggesting that Src activation both preceded and was obligatory for RhoA activation.

Stress fiber formation can occur as a consequence of Erk-mediated tropomyosin phosphorylation [Houle et al., 2007]. To uncover any potential role for Erk in cholesterol-depletion induced stress fiber formation we first tested whether Erk is phosphorylated (activated) as a consequence of MβCD treatment (Fig. 6A). Based on immunoblotting, we determined that Erk was phosphorylated after exposure to MβCD. We next assessed whether we could inhibit Erk phosphorylation in response to cholesterol-depletion by treating cells with U0126, an inhibitor of Mek, the kinase lying immediately upstream of Erk (Fig. 6B). Based on immunoblot analysis of Erk phosphorylation, we determined that U0126 treatment completely blocked MβCD induced phosphorylation of Erk (compare lanes 2 vs. 6 in Fig. 6B). In contrast, treating cells with U0126 had little to no effect on MβCD treatment-induced phosphorylation of caveolin or on stress fiber formation (data not shown). Disassembly of the actin cytoskeleton with latrunculin A (LAT A), which binds to G-actin and disassembles actin filaments, did not reduce the ability of MβCD to induce Erk phosphorylation

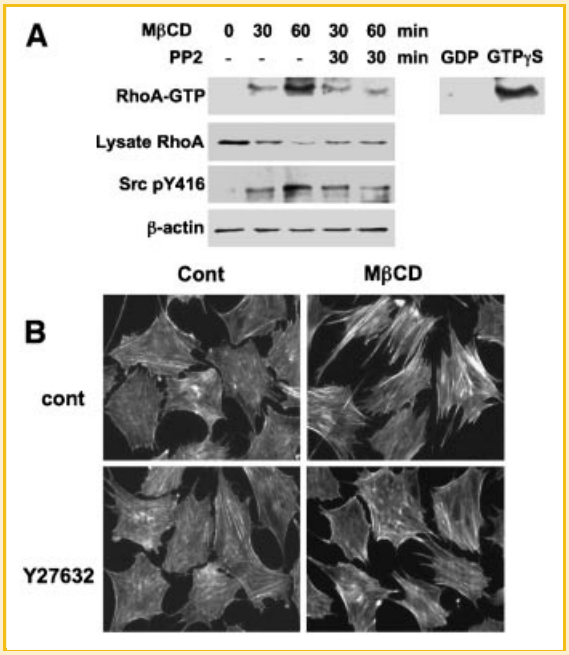

Fig. 4. RhoA signaling is required for stress fiber formation mediated by cholesterol depletion. A: RhoA is activated by MβCD. Serum-starved MC3T3 cells were treated with 5 mM of MβCD for 0, 30, and 60 min in the absence or presence of 10 μM of PP2. Activation of RhoA was assessed by a Rho-RBD pull down assay as described in Materials and Methods Section. The amount of RhoA-GTP was detected by blotting the precipitates with an anti-RhoA antibody. The total levels of RhoA and Src pY416 were examined by immunoblotting the whole cell lysates. Immunoblotting for β-actin was used as loading control. B: Rho kinase inhibition blocks MβCD-induced stress fiber formation. MC3T3 cells were seeded onto coverslips in 3-cm dishes and cultured 1–2 days and then serum starved over night. Cells were treated with either vehicle or 2.5 μM Rho-kinase (ROCK) inhibitor Y-27632 for 30 min and then with either vehicle or 5 mM MβCD for 30 min. After treatment, cells were fixed with 4% paraformaldehyde and permeablized in 0.1% Triton X-100 and stained with rhodamine-phalloidin to visualize stress fibers.

(Fig. 6B, lanes 3 and 4). Taken together these data suggest that Erk activation is not required for, nor is the result of, stress fiber formation.

DISCUSSION

Cholesterol is a major component of eukaryotic cell membranes, with important effects on membrane fluidity, stiffness, and compartmentalization. Altering membrane cholesterol levels affects many cell processes including signal transduction mechanisms, molecular transport, cell morphology, as well as the distribution of proteins and lipids in the plane of the membrane. All of these processes to which cholesterol contributes necessarily involve one or more aspects of the cytoskeleton, however the role cholesterol plays in regulating the membrane-cytoskeleton interaction has not been established. Here we show that membrane cholesterol regulates the formation of actin stress fibers through a process that requires Rho, ROCK, Src, and Cav1.

Relatively few studies have looked at cholesterol's role in F-actin assembly. In studies looking at sperm capacitation, it was demonstrated that the assembly of F-actin requires the introduction of cyclodextrin to sperm cultures, suggesting that cholesterol depletion is obligatory for actin polymerization during capacitation [Brener et al., 2003]. Other studies using the human leukemia cell line K562 demonstrated that cholesterol depletion using cyclodextrin causes a loss of cortical actin and a redistribution/accumulation of F-actin in the cytoplasm [Morachevskaya et al., 2007]. In contrast, Klausen et al. [2006] showed that cyclodextrin-mediated cholesterol depletion causes F-actin polymerization, a finding consistent with a prior report describing F-actin-mediated stiffening of aortic endothelial cells following cholesterol depletion [Byfield et al., 2004].

There are fewer studies directly addressing the role of cholesterol in stress fiber formation, and these have produced conflicting accounts. Kwik et al. [2003] report that cholesterol depletion *prevents* stress fiber formation, while Klausen et al. [2006] report that cholesterol depletion *triggers* stress fiber formation, this latter report being consistent with the studies reported here. Kwik et al. used non-transformed fibroblasts, Klausen et al. used Ehrlick ascites tumor (EAT) cells, and in our current study we have used two cell types: MC3T3 murine osteoblasts and PC3 human prostatic adenocarcinoma cells. Why Kwik et al. using non-transformed fibroblasts obtained results disparate from those obtained by Klausen et al. and contained herein is not known. Possible explanations include differences in normal cholesterol levels, affects of lesser or greater amount of cholesterol depletion, the level of pre-existing stress fibers, and the activation state of signaling intermediates. Both of these prior reports used MβCD to deplete cholesterol, as was done here, suggesting that the noted differences in the manner that cholesterol depletion effects the different cell types used is not a function of method of cholesterol depletion, per se.

A 1 h treatment with 5 mM MβCD causes a ≈30–50% depletion of cholesterol ([Klausen et al., 2006] and data not shown), a dramatic change in cholesterol level that is actually quite similar to the difference in cholesterol levels found between tissues in normocholesterolemic and hypercholesterolemic mice [Dvornik and Hill, 1968], suggesting that cholesterol level modulation by MβCD treatment mimics biologically relevant alterations in tissue cholesterol level.

Caveolin is phosphorylated on tyrosine-14 [Lee et al., 2000], and its induced phosphorylation occurs at or near focal adhesions (FA) [Volonte et al., 2001; del Pozo et al., 2004; Swaney et al., 2006]. Ventral stress fibers, (the most commonly observed stress fibers) attach to integrin-rich FA on both fiber ends [Burridge, 1986], while dorsal stress fibers are tethered on only one end to the FA [Heath and Dunn, 1978]. Thus, given that both stress fibers and p-Cav1 are found in FA it is anticipated that stress fibers and p-Cav1 would co-localize. In fact, prior studies have shown that the formation of actin stress fibers is associated with a redistribution of phosphorylated caveolin from internal sites to focal adhesions [Beardsley et al., 2005; Swaney et al., 2006], where it co-localizes with the ends of the actin stress fibers. Studies from our lab demonstrate that ablation of Cav1 α (which contains Y-14) and β (which does not have Y-14) in

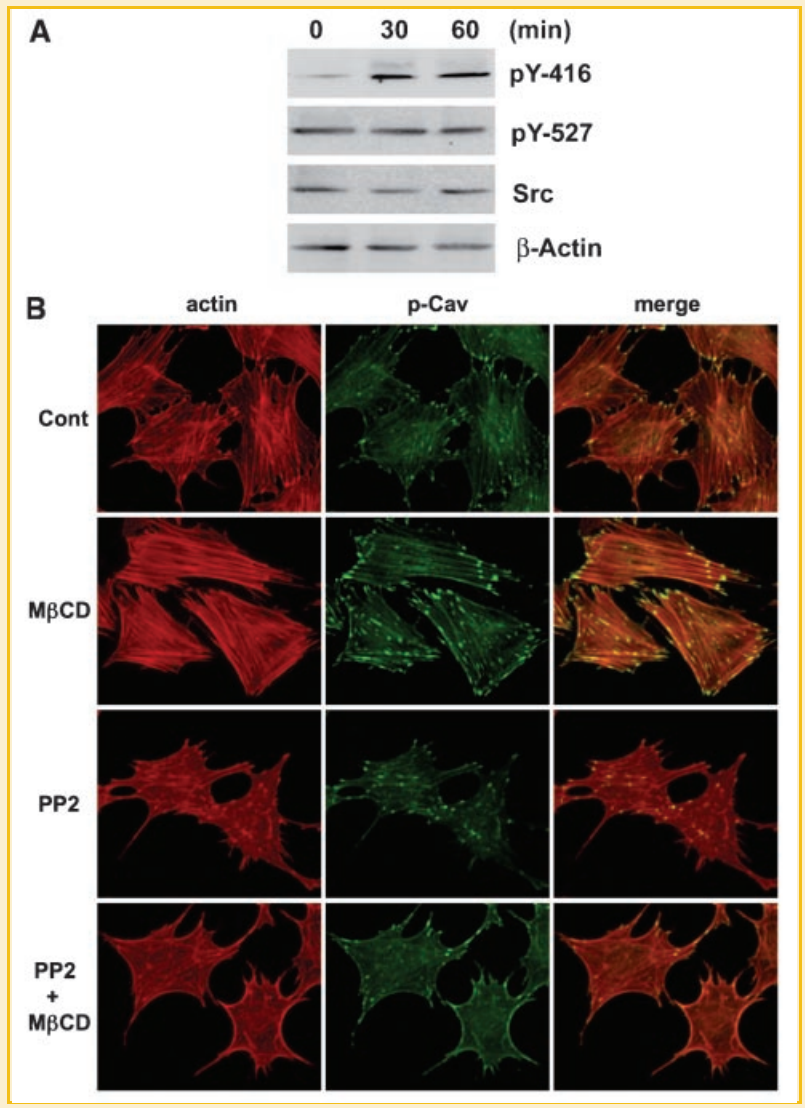

Fig. 5. Src is required for cholesterol-depletion induced stress fiber formation. A: Src is activated by MβCD treatment. MC3T3 cells were starved and treated with 5 mM MβCD for 0, 30, and 60 min. Cells were then washed with cold PBS and lysed in RIPA buffer. Forty micrograms of total protein of each lysate was subjected to immunoblot analysis with polyclonal anti-pY416-Src, anti-pY527-Src, anti-total Src or β-actin. B: Src inhibition reduces MβCD-induced Cav1 redistribution and stress fiber formation. MC3T3 cells were serum-starved and treated with 10 μM PP2 or mock treated for 30 min and then treated with 5 mM MβCD or mock treated for 30 min. Monoclonal anti-phospho-caveolin was then added and incubated for 90 min at RT. After washing with PBS, FITC-coupled goat anti-rabbit reporter antibody plus rhodamine-phalloidin were added and incubated in dark for 60 min.

the zebrafish results in embryonic lethality coinciding with a disorganized (collapsed) actin-based cytoskeleton [Fang et al., 2006]. Neither the embryonic lethality nor the disrupted actin cytoskeleton are rescued by Cav1 α that carries a Y → A mutation at position 14, suggesting that Cav1 phosphorylation is critical for the integrity of the actin cytoskeleton [Fang et al., 2006], consistent with the observations reported here. The studies described in our current report demonstrate that the formation of stress fibers and the location of p-caveolin at their ends are not simply coincident events but that tyrosine phosphorylation of Cav1 is requisite for stress fiber formation. This conclusion is suggested by results derived using two distinct methods: First, we show that MβCD-induced stress fiber formation requires caveolin (as determined by siRNA-mediated Cav1 knockdown) (Fig. 3B) and second, that it requires Src family kinase activity (Figs. 4A and 5). To our knowledge, these are the first results that suggest that Cav1 phosphorylation is *obligatory* for stress fiber formation.

Caveolin was first identified as a tyrosine phosphorylated protein in v-Src transformed cells [Glenney and Zokas, 1989; Glenney and Soppet, 1992], and subsequent studies have shown that Src phosphorylates Cav1, which regulates c-Src activity [Li et al., 1996a]. Our results using the Src kinase inhibitor PP2 suggest that Src kinase activity is required for Cav1 phosphorylation, and the subsequent formation of stress fibers. Although v-Src and c-Src are known to phosphorylate Cav1, other Src family tyrosine kinases do so as well [Sanguinetti et al., 2003]. The Src kinase inhibitor PP2

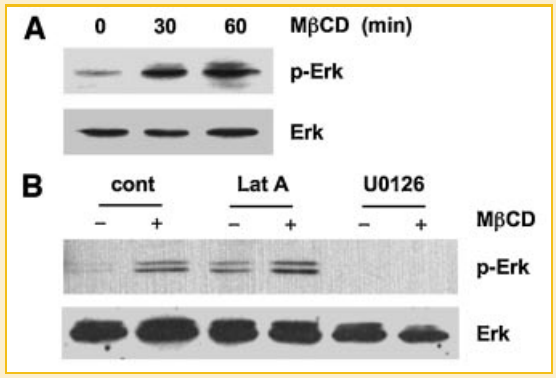

Fig. 6. MβCD-induced increases in Erk phosphorylation are not the result of stress fiber formation. A: MβCD-induced Erk phosphorylation. MC3T3 cells grown in 3-cm cell culture dishes were starved and treated with 5 mM MβCD for 0, 30, and 60 min. Cells were then washed with cold PBS and lysed in RIPA buffer. Thirty micrograms of total protein of each sample was resolved by SDS–PAGE using a 10% polyacrylamide gel and then electrotransferred to a nitrocellulose membrane. Erk phosphorylation was monitored by blotting sequentially with monoclonal anti-phospho-Erk and HRP-coupled anti-mouse reporter antibody, followed by stripping and reprobing with an anti-Erk antibody. B: Actin disassembly does not block Erk phosphorylation. MC3T3 cells were treated with 10 μM U0126 or 2.5 μM Lat A (or vehicle) for 30 min prior to treatment with 5 mM MβCD (or mock treated) for 30 min. Cell lysates were subjected to SDS-PAGE and immunoblotting as described above in part A.

affects the activity of Src as well as that of other Src kinase family member, so the use of this inhibitor does not reveal the identity of the phosphorylating species. Thus, prior reports demonstrating that c-Src activation inhibits stress fiber formation and/or causes their disassembly [Chang et al., 1995; Haskell et al., 2001; Pawlak and Helfman, 2002] and our current one are not necessarily contradictory. Moreover, activation of heterotrimeric G proteins leads to stress fiber formation via a Rho activation mechanism sensitive to tyrosine kinase inhibitors [Lowry et al., 2002]. Overall, our current results suggest that cholesterol-depletion sensitive stress fiber assembly is quite similar to stress fiber formation induced by heterotrimeric G protein activation.

Another interesting observation made here is that cholesterol depletion increases the level of GTP bound RhoA, while also reducing the total level of RhoA. The activation of RhoA is mediated by a number of interacting molecules, including guanine nucleotide exchange factors (GEFs), that participate in the activation of membrane attached, prenylated RhoA. Inactive RhoA, either GDP-bound or nucleotide free, which cycles from the membrane to the cytosol is targeted for ubiquitination and proteolysis by the E3 ligase, Smurf1 [Wang et al., 2003; Rossman et al., 2005; Wang et al., 2006]. Although we do not know why cholesterol depletion leads to a loss of total RhoA, we speculate that removing cholesterol from the plasma membrane reduces the sites for prenylated RhoA-membrane interaction, causing a fraction of RhoA to be released from the membrane, which subsequently becomes a target for ubiquitination and degradation.

In our studies, we demonstrate that cholesterol depletion induces stress fiber formation, suggesting that membrane cholesterol has a regulatory function with regards to actin polymerization. Since stress fiber formation is a necessary response to the application of mechanical forces to cells, alteration of stress fibers through cholesterol modulation may result in aberrant responses to mechanical signals. Cholesterol depletion has been shown to disrupt mechanotransduction, but the mechanism of this effect is obscure [Ferraro et al., 2004; Potocnik et al., 2007; Radel et al., 2007]. One possibility, consistent with the evidence presented here, is that cholesterol depletion causes aberrant (premature?) stress fiber formation resulting in a substantially blunted response to sheer and strain forces. Given that the cellular responses to mechanical stimulation is critical for the maintenance of various tissues (for example osteoblastic bone maintenance), our results suggest the possibility that altered membrane cholesterol levels may significantly affect mechanotransduction and thereby compromise health.

We propose that cholesterol depletion induces Src kinase activation leading to RhoA activation and subsequently to ROCK activation, and actin polymerization, resulting ultimately in stress fiber formation (Fig. 7). Src kinase family members are known to be highly enriched in lipid raft microdomains, thus it is possible that by depleting the cells of cholesterol we are directly affecting Src kinases, which become activated and trigger the signaling cascade. Alternatively, depleting cholesterol may trigger the activation of a membrane sensitive signaling component (e.g., a heterotrimeric G protein) which then transactivates the Src kinases to trigger the actin polymerization required for stress fiber formation.

In conclusion, we have demonstrated that membrane cholesterol concentration influences actin polymerization to the degree that acute cholesterol depletion results in stress fiber formation. We hypothesize that membrane cholesterol through its role in regulating the actin cytoskeleton may alter the ability of cells to respond to physiological stress potentially resulting in aberrant behavior in response to mechanical signals. Many cell types are required to respond appropriately to mechanical signals, thus our results obtained using osteoblasts, and prostate carcinoma cells, may be relevant to other cell types as well.

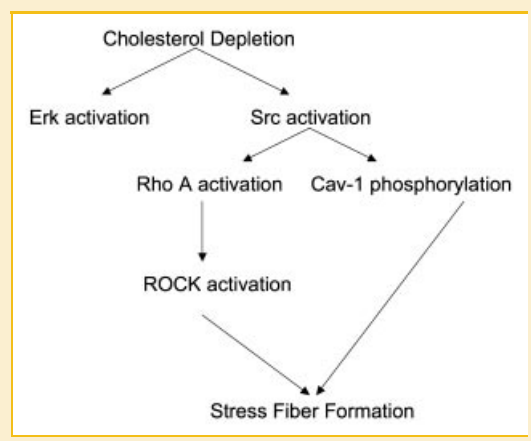

Fig. 7. Hypothesized signaling pathway leading to stress fiber formation from membrane cholesterol depletion.

ACKNOWLEDGMENTS

The authors would like to thank Dolores Di Vizio, Donald Ingber, and Marsha Moses for their advice and critical reading of the manuscript. National Institutes of Health (CA101046 to K.R.S.).

REFERENCES

Baron W, Decker L, Colognato H, Ffrench-Constant C. 2003. Regulation of integrin growth factor interactions in oligodendrocytes by lipid raft microdomains. Curr Biol 13:151–155.

Beardsley A, Fang K, Mertz H, Castranova V, Friend S, Liu J. 2005. Loss of caveolin-1 polarity impedes endothelial cell polarization and directional movement. J Biol Chem 280:3541–3547.

Brener E, Rubinstein S, Cohen G, Shternall K, Rivlin J, Breitbart H. 2003. Remodeling of the actin cytoskeleton during mammalian sperm capacitation and acrosome reaction. Biol Reprod 68:837–845.

Burridge K. 1986. Substrate adhesions in normal and transformed fibroblasts: Organization and regulation of cytoskeletal, membrane, and extracellular matrix components at focal contacts. Cancer Rev 4:18–78.

Byfield FJ, Aranda-Espinoza H, Romanenko VG, Rothblat GH, Levitan I. 2004. Cholesterol depletion increases membrane stiffness of aortic endothelial cells. Biophys J 87:3336–3343.

Chang JH, Gill S, Settleman J, Parsons SJ. 1995. c-Src regulates the simultaneous rearrangement of actin cytoskeleton, p190RhoGAP, and p120RasGAP following epidermal growth factor stimulation. J Cell Biol 130:355–368.

Conrad PA, Smart EJ, Ying YS, Anderson RG, Bloom GS. 1995. Caveolin cycles between plasma membrane caveolae and the Golgi complex by microtubule-dependent and microtubule-independent steps. J Cell Biol 131:1421–1433.

del Pozo MA, Alderson NB, Kiosses WB, Chiang HH, Anderson RG, Schwartz MA. 2004. Integrins regulate Rac targeting by internalization of membrane domains. Science 303:839–842.

Dvornik D, Hill P. 1968. Effect of long-term administration of AY-9944, an inhibitor of 7-dehydrocholesterol delta 7-reductase, on serum and tissue lipids in the rat. J Lipid Res 9:587–595.

Fang PK, Solomon KR, Zhuang L, Qi M, McKee M, Freeman MR, Yelick PC. 2006. Caveolin-1alpha and -1beta perform nonredundant roles in early vertebrate development. Am J Pathol 169:2209–2222.

Faure C, Linossier MT, Malaval L, Lafage-Proust MH, Peyroche S, Vico L, Guignandon A. 2008. Mechanical signals modulated vascular endothelial growth factor-A (VEGF-A) alternative splicing in osteoblastic cells through actin polymerisation. Bone 42:1092–1101.

Ferraro JT, Daneshmand M, Bizios R, Rizzo V. 2004. Depletion of plasma membrane cholesterol dampens hydrostatic pressure and shear stress-induced mechanotransduction pathways in osteoblast cultures. Am J Physiol Cell Physiol 286:C831–C839.

Frank PG, Cheung MW, Pavlides S, Llaverias G, Park DS, Lisanti MP. 2006. Caveolin-1 and regulation of cellular cholesterol homeostasis. Am J Physiol Heart Circ Physiol 291:H677–H686.

Glenney JR Jr, Soppet D. 1992. Sequence and expression of caveolin, a protein component of caveolae plasma membrane domains phosphorylated on tyrosine in Rous sarcoma virus-transformed fibroblasts. Proc Natl Acad Sci USA 89:10517–10521.

Glenney JR Jr, Zokas L. 1989. Novel tyrosine kinase substrates from Rous sarcoma virus-transformed cells are present in the membrane skeleton. J Cell Biol 108:2401–2408.

Gomez-Mouton C, Abad JL, Mira E, Lacalle RA, Gallardo E, Jimenez-Baranda S, Illa I, Bernad A, Manes S, Martinez AC. 2001. Segregation of leading-edge and uropod components into specific lipid rafts during T cell polarization. Proc Natl Acad Sci USA 98:9642–9647.

Green JM, Zhelesnyak A, Chung J, Lindberg FP, Sarfati M, Frazier WA, Brown EJ. 1999. Role of cholesterol in formation and function of a signaling complex involving alphavbeta3, integrin-associated protein (CD47), and heterotrimeric G proteins. J Cell Biol 146:673–682.

Haskell MD, Nickles AL, Agati JM, Su L, Dukes BD, Parsons SJ. 2001. Phosphorylation of p190 on Tyr1105 by c-Src is necessary but not sufficient for EGF-induced actin disassembly in C3H10T1/2 fibroblasts. J Cell Sci 114:1699–1708.

Heath JP, Dunn GA. 1978. Cell to substratum contacts of chick fibroblasts and their relation to the microfilament system. A correlated interference-reflexion and high-voltage electron-microscope study. J Cell Sci 29:197–212.

Hocking DC, Kowalski K. 2002. A cryptic fragment from fibronectin's III1 module localizes to lipid rafts and stimulates cell growth and contractility. J Cell Biol 158:175–184.

Houle F, Poirier A, Dumaresq J, Huot J. 2007. DAP kinase mediates the phosphorylation of tropomyosin-1 downstream of the ERK pathway, which regulates the formation of stress fibers in response to oxidative stress. J Cell Sci 120:3666–3677.

Hughes-Fulford M. 2004. Signal transduction and mechanical stress. Sci STKE 2004:RE12.

Klausen TK, Hougaard C, Hoffmann EK, Pedersen SF. 2006. Cholesterol modulates the volume-regulated anion current in Ehrlich-Lettre ascites cells via effects on Rho and F-actin. Am J Physiol Cell Physiol 291:C757–C771.

Kwik J, Boyle S, Fooksman D, Margolis L, Sheetz MP, Edidin M. 2003. Membrane cholesterol, lateral mobility, and the phosphatidylinositol 4,5-bisphosphate-dependent organization of cell actin. Proc Natl Acad Sci USA 100:13964–13969.

Labrecque L, Nyalendo C, Langlois S, Durocher Y, Roghi C, Murphy G, Gingras D, Beliveau R. 2004. Src-mediated tyrosine phosphorylation of caveolin-1 induces its association with membrane type 1 matrix metalloproteinase. J Biol Chem 279:52132–52140.

Lee H, Volonte D, Galbiati F, Iyengar P, Lublin DM, Bregman DB, Wilson MT, Campos-Gonzalez R, Bouzahzah B, Pestell RG, Scherer PE, Lisanti MP. 2000. Constitutive and growth factor-regulated phosphorylation of caveolin-1 occurs at the same site (Tyr-14) in vivo: Identification of a c-Src/Cav-1/Grb7 signaling cassette. Mol Endocrinol 14:1750–1775.

Lee H, Park DS, Razani B, Russell RG, Pestell RG, Lisanti MP. 2002. Caveolin-1 mutations (P132L and null) and the pathogenesis of breast cancer: Caveolin-1 (P132L) behaves in a dominant-negative manner and caveolin-1 (−/−) null mice show mammary epithelial cell hyperplasia. Am J Pathol 161:1357–1369.

Leitinger B, Hogg N. 2002. The involvement of lipid rafts in the regulation of integrin function. J Cell Sci 115:963–972.

Li S, Couet J, Lisanti MP. 1996a. Src tyrosine kinases, Galpha subunits, and H-Ras share a common membrane-anchored scaffolding protein, caveolin. Caveolin binding negatively regulates the auto-activation of Src tyrosine kinases. J Biol Chem 271:29182–29190.

Li S, Seitz R, Lisanti MP. 1996b. Phosphorylation of caveolin by src tyrosine kinases. The alpha-isoform of caveolin is selectively phosphorylated by v-Src in vivo. J Biol Chem 271:3863–3868.

Lillemeier BF, Pfeiffer JR, Surviladze Z, Wilson BS, Davis MM. 2006. Plasma membrane-associated proteins are clustered into islands attached to the cytoskeleton. Proc Natl Acad Sci USA 103:18992–18997.

Lowry WE, Huang J, Ma YC, Ali S, Wang D, Williams DM, Okada M, Cole PA, Huang XY. 2002. Csk, a critical link of g protein signals to actin cytoskeletal reorganization. Dev Cell 2:733–744.

MacLellan DL, Steen H, Adam RM, Garlick M, Zurakowski D, Gygi SP, Freeman MR, Solomon KR. 2005. A quantitative proteomic analysis of growth factor-induced compositional changes in lipid rafts of human smooth muscle cells. Proteomics 5:4733–4742.

Manes S, Lacalle RA, Gomez-Mouton C, del Real G, Mira E, Martinez AC. 2001. Membrane raft microdomains in chemokine receptor function. Semin Immunol 13:147–157.

Maxfield FR. 2002. Plasma membrane microdomains. Curr Opin Cell Biol 14:483–487.

McGarry JG, Klein-Nulend J, Prendergast PJ. 2005. The effect of cytoskeletal disruption on pulsatile fluid flow-induced nitric oxide and prostaglandin E2 release in osteocytes and osteoblasts. Biochem Biophys Res Commun 330: 341–348.

Meazzini MC, Toma CD, Schaffer JL, Gray ML, Gerstenfeld LC. 1998. Osteoblast cytoskeletal modulation in response to mechanical strain in vitro. J Orthop Res 16:170–180.

Michaely PA, Mineo C, Ying YS, Anderson RG. 1999. Polarized distribution of endogenous Rac1 and RhoA at the cell surface. J Biol Chem 274:21430–21436.

Morachevskaya E, Sudarikova A, Negulyaev Y. 2007. Mechanosensitive channel activity and F-actin organization in cholesterol-depleted human leukaemia cells. Cell Biol Int 31:374–381.

Mukherjee S, Maxfield FR. 2004. Membrane domains. Annu Rev Cell Dev Biol 20:839–866.

Murata M, Peranen J, Schreiner R, Wieland F, Kurzchalia TV, Simons K. 1995. VIP21/caveolin is a cholesterol-binding protein. Proc Natl Acad Sci USA 92:10339–10343.

Naal RM, Holowka EP, Baird B, Holowka D. 2003. Antigen-stimulated trafficking from the recycling compartment to the plasma membrane in RBL mast cells. Traffic 4:190–200.

Park DS, Woodman SE, Schubert W, Cohen AW, Frank PG, Chandra M, Shirani J, Razani B, Tang B, Jelicks LA, Factor SM, Weiss LM, Tanowitz HB, Lisanti MP. 2002. Caveolin-1/3 double-knockout mice are viable, but lack both muscle and non-muscle caveolae, and develop a severe cardiomyopathic phenotype. Am J Pathol 160:2207–2217.

Pawlak G, Helfman DM. 2002. MEK mediates v-Src-induced disruption of the actin cytoskeleton via inactivation of the Rho-ROCK-LIM kinase pathway. J Biol Chem 277:26927–26933.

Pellegrin S, Mellor H. 2007. Actin stress fibres. J Cell Sci 120:3491–3499.

Potocnik SJ, Jenkins N, Murphy TV, Hill MA. 2007. Membrane cholesterol depletion with beta-cyclodextrin impairs pressure-induced contraction and calcium signalling in isolated skeletal muscle arterioles. J Vasc Res 44:292–302.

Radel C, Carlile-Klusacek M, Rizzo V. 2007. Participation of caveolae in beta1 integrin-mediated mechanotransduction. Biochem Biophys Res Commun 358:626–631.

Rossman KL, Der CJ, Sondek J. 2005. GEF means go: Turning on RHO GTPases with guanine nucleotide-exchange factors. Nat Rev Mol Cell Biol 6:167–180.

Sanguinetti AR, Cao H, Corley Mastick C. 2003. Fyn is required for oxidative- and hyperosmotic-stress-induced tyrosine phosphorylation of caveolin-1. Biochem J 376:159–168.

Scott A, Khan KM, Duronio V, Hart DA. 2008. Mechanotransduction in human bone: In vitro cellular physiology that underpins bone changes with exercise. Sports Med 38:139–160.

Simons K, Vaz WL. 2004. Model systems, lipid rafts, and cell membranes. Annu Rev Biophys Biomol Struct 33:269–295.

Skubitz KM, Campbell KD, Skubitz AP. 2000. CD63 associates with CD11/CD18 in large detergent-resistant complexes after translocation to the cell surface in human neutrophils. FEBS Lett 469:52–56.

Sleer LS, Brown AJ, Stanley KK. 2001. Interaction of caveolin with 7-ketocholesterol. Atherosclerosis 159:49–55.

Smart EJ, Ying YS, Conrad PA, Anderson RG. 1994. Caveolin moves from caveolae to the Golgi apparatus in response to cholesterol oxidation. J Cell Biol 127:1185–1197.

Sudo H, Kodama HA, Amagai Y, Yamamoto S, Kasai S. 1983. In vitro differentiation and calcification in a new clonal osteogenic cell line derived from newborn mouse calvaria. J Cell Biol 96:191–198.

Sun M, Northup N, Marga F, Huber T, Byfield FJ, Levitan I, Forgacs G. 2007. The effect of cellular cholesterol on membrane-cytoskeleton adhesion. J Cell Sci 120:2223–2231.

Swaney JS, Patel HH, Yokoyama U, Head BP, Roth DM, Insel PA. 2006. Focal adhesions in (myo)fibroblasts scaffold adenylyl cyclase with phosphorylated caveolin. J Biol Chem 281:17173–17179.

Thorne RF, Marshall JF, Shafren DR, Gibson PG, Hart IR, Burns GF. 2000. The integrins alpha3beta1 and alpha6beta1 physically and functionally associate with CD36 in human melanoma cells. Requirement for the extracellular domain OF CD36. J Biol Chem 275:35264–35275.

Thyberg J, Roy J, Tran PK, Blomgren K, Dumitrescu A, Hedin U. 1997. Expression of caveolae on the surface of rat arterial smooth muscle cells is dependent on the phenotypic state of the cells. Lab Invest 77:93–101.

Uittenbogaard A, Smart EJ. 2000. Palmitoylation of caveolin-1 is required for cholesterol binding, chaperone complex formation, and rapid transport of cholesterol to caveolae. J Biol Chem 275:25595–25599.

van Deurs B, Roepstorff K, Hommelgaard AM, Sandvig K. 2003. Caveolae: Anchored, multifunctional platforms in the lipid ocean. Trends Cell Biol 13:92–100.

Volonte D, Galbiati F, Pestell RG, Lisanti MP. 2001. Cellular stress induces the tyrosine phosphorylation of caveolin-1 (Tyr(14)) via activation of p38 mitogen-activated protein kinase and c-Src kinase. Evidence for caveolae, the actin cytoskeleton, and focal adhesions as mechanical sensors of osmotic stress. J Biol Chem 276:8094–8103.

Wang HR, Zhang Y, Ozdamar B, Ogunjimi AA, Alexandrova E, Thomsen GH, Wrana JL. 2003. Regulation of cell polarity and protrusion formation by targeting RhoA for degradation. Science 302:1775–1779.

Wang HR, Ogunjimi AA, Zhang Y, Ozdamar B, Bose R, Wrana JL. 2006. Degradation of RhoA by Smurf1 ubiquitin ligase. Methods Enzymol 406: 437–447.

Woodman SE, Park DS, Cohen AW, Cheung MW, Chandra M, Shirani J, Tang B, Jelicks LA, Kitsis RN, Christ GJ, Factor SM, Tanowitz HB, Lisanti MP. 2002. Caveolin-3 knock-out mice develop a progressive cardiomyopathy and show hyperactivation of the p42/44 MAPK cascade. J Biol Chem 277:38988–38997.

Zhang B, Peng F, Wu D, Ingram AJ, Gao B, Krepinsky JC. 2007. Caveolin-1 phosphorylation is required for stretch-induced EGFR and Akt activation in mesangial cells. Cell Signal 19:1690–1700.